Systems/Circuits

Existence of a Long-Range Caudo-Rostral Sensory Influence in Terrestrial Locomotion

Martyna Grabowska,[1] Tibor I. Toth,[1] Ansgar Büschges,[1,3] and Silvia Daun[1,2]

[1]Institute of Zoology, University of Cologne, Cologne 50674, Germany, [2]Cognitive Neuroscience, Institute of Neuroscience and Medicine (INM-3), Research Centre Jülich, Jülich 52428, Germany, and [3]Department of Animal Physiology, Institute of Zoology, University of Cologne, Cologne 50674, Germany

In multisegmented locomotion, coordination of all appendages is crucial for the generation of a proper motor output. In running for example, leg coordination is mainly based on the central interaction of rhythm generating networks, called central pattern generators (CPGs). In slower forms of locomotion, however, sensory feedback, which originates from sensory organs that detect changes in position, velocity and load of the legs' segments, has been shown to play a more crucial role. How exactly sensory feedback influences the activity of the CPGs to establish functional neuronal connectivity is not yet fully understood. Using the female stick insect *Carausius morosus*, we show for the first time that a long-range caudo-rostral sensory connection exists and highlight that load as sensory signal is sufficient to entrain rhythmic motoneuron (MN) activity in the most rostral segment. So far, mainly rostro-caudal influencing pathways have been investigated where the strength of activation, expressed by the MN activity in the thoracic ganglia, decreases with the distance from the stepping leg to these ganglia. Here, we activated CPGs, producing rhythmic neuronal activity in the thoracic ganglia by using the muscarinic agonist pilocarpine and enforced the stepping of a single, remaining leg. This enabled us to study sensory influences on the CPGs' oscillatory activity. Using this approach, we show that, in contrast to the distance-dependent activation of the protractor-retractor CPGs in different thoracic ganglia, there is no such dependence for the entrainment of the rhythmic activity of active protractor-retractor CPG networks by individual stepping legs.

Key words: **six-legged walking; CPG; entrainment; inter-segmental coordination; locomotion**

Significance Statement

We show for the first time that sensory information is transferred not only to the immediate adjacent segmental ganglia but also to those farther away, indicating the existence of a long-range caudo-rostral sensory influence. This influence is dependent on stepping direction but independent of whether the leg is actively or passively moved. We suggest that the sensory information comes from unspecific load signals sensed by cuticle mechanoreceptors (campaniform sensilla) of a leg. Our results provide a neuronal basis for the long-established behavioral rules of insect leg coordination. We thus provide a breakthrough in understanding the neuronal networks underlying multilegged locomotion and open new vistas into the neuronal functional connectivity of multisegmented locomotion systems across the animal kingdom.

Introduction

One of the most challenging tasks in understanding locomotion is to identify neuronal networks that shape the coordination of all appendages in multisegmented animals. Running (Fuchs et al., 2011; David et al., 2016; Grillner and El Manira, 2020), for example, has been found to be based on the interaction of rhythm generating networks in the central nervous system, so called central pattern generators (CPGs), and can occur with little or no sensory feedback (Grillner and Wallén, 1985; Katz, 2016). Slower forms of terrestrial locomotion, like walking, however, require sensory modulation to instantaneously adapt movements to environmental irregularities. These kinds of locomotion have been particularly studied in insects (Sponberg and Full, 2008; Ritzmann and Zill, 2013; Knebel et al., 2017; Schilling and Cruse, 2020). Locomotor systems consist of multiple CPGs within and across body segments that need to be coordinated. The functional connectivity between nonadjacent body segments that influences the activity of these CPGs via sensory input is, however, still poorly understood and will be studied here.

Received Sep. 1, 2020; revised Apr. 21, 2022; accepted Apr. 22, 2022.

Author contributions: S.D. designed research; M.G. performed research; M.G., T.I.T., A.B., and S.D. contributed unpublished reagents/analytic tools; M.G. analyzed data; M.G. wrote the first draft of the paper; T.I.T., A.B., and S.D. edited the paper; M.G., T.I.T., and S.D. wrote the paper.

This work was supported by the Deutsche Forschungsgemeinschaft (DFG, German Research Foundation) Grants Project-ID 431549029–SFB 1451 and 491111487. S.D. was also supported by DFG Grants DA1953/5-2 and DA1953/4-2.

The authors declare no competing financial interests.

Correspondence should be addressed to Silvia Daun at s.daun@fz-juelich.de.

https://doi.org/10.1523/JNEUROSCI.2290-20.2022

Bi-directional functional long-range and short-range connections have been described in orthopteran flight, where synchrony of beating of forewings and hindwings is generated by a CPG network distributed among the thoracic ganglia (Ronacher et al., 1988), as well as in the neurally mediated coupling in the generation of the motor output for swimming (leech, Cang and Friesen, 2002; lamprey, Grillner, 2006), crawling (leech, Puhl and Mesce, 2008) and the swimmeret movements of crustaceans (Smarandache-Wellmann and Grätsch, 2014). Terrestrial locomotion in arthropods, on the other hand, describes a variety of speed dependent inter-leg coordination patterns such as a slow metachronal wave pattern or a fast tripod coordination pattern (Graham, 1981; Grabowska et al., 2012; Wosnitza et al., 2013). Coordination rules between neighboring legs have been identified based on mechanical (not neural) properties of the insect's body (Cruse, 1990; Schilling et al., 2013) and allow for an explanation of the generation of these coordination pattern. For the slow walking stick insect, it is known that CPGs of the thoracic ganglia are only weakly coupled, and without sensory feedback this coupling is insufficient to produce leg coordination observed behaviorally (Mantziaris et al., 2017). Knowledge on sensory pathways, which may transmit neuronal information between nonadjacent legs, is thus still limited.

In insect walking, neuronal connections between stepping legs have been mostly studied for a rostro-caudal direction, including the role of sensory signals: Studies in tethered stick insects showed that stepping front legs activate the protractor-retractor motoneurons (MNs) in the mesothoracic ganglion and entrain their periodic activities, leading to in-phase rhythmic discharges of prothoracic and mesothoracic protractor and retractor MNs (Borgmann et al., 2009). MNs in the metathoracic ganglion, however, were only rhythmically active in-phase on induction of rhythmic motor activity in both rostral segments, indicating a hierarchical influence on the other thoracic CPGs in rostro-caudal direction, with the most adjacent segments being affected the strongest by a walking leg (Ludwar et al., 2005; Borgmann et al., 2007, 2009).

A slow walking sequence in hexapod locomotion, where the hind leg is starting a sequence of consecutive leg swing phases from caudal to rostral (Grabowska et al., 2012), could indicate a functional, ipsilateral connection that propagates coordinating signals arising from sensory organs from most posterior thoracic segments. Nonetheless, the existence of such long-range caudo-rostral neural influences of an insect's stepping hind leg on the prothoracic CPGs has yet not been shown. Such connection was found to be crucial for generating coordinated leg movements of all legs in mathematical models reproducing neuronal activity of stick insect locomotion (Daun-Gruhn and Tóth, 2011; Toth et al., 2015; Tóth and Daun, 2019). Here, we present experimental evidence for the existence of a functional long-range caudo-rostral sensory connection and confirm that load as sensory signal is sufficient to entrain pharmacologically activated CPG activity in the most rostral segment. Interestingly, the entraining effect is not dependent on the distance from the origin of the sensory signals caused by leg movements.

Materials and Methods

Animals

Female adult stick insects, *Carausius morosus*, were used from the breed of the Zoological Institute at the University of Cologne. The animals were kept at room temperature (18–22°C) at a 12/12 h light/dark cycle.

Electrophysiological experiments

The basic arrangement for all experiments was a semi-intact preparation. In all cases, the stick insect was pinned dorsal side up to a foam platform. All legs, except one (left front, middle, or hind leg), were cut at mid-coxa level and the stumps were also fixated to the foam platform with insect pins. The thorax of the stick insect was opened with a sagittal cut along the midline of the cuticle from the most rostral point of the prothorax to the most caudal side of the mesothoracic ganglion, just before the beginning of the metathoracic ganglion. The gut, as well as the connective tissue, was removed to expose the ganglia of interest, their connectives, and their lateral leg nerves. A u-shaped portion of the cuticle was removed to place a vaseline barrier between the segments to avoid mixing of the different solutions in the cavities (Borgmann et al., 2009). The segment with the intact leg remained closed and was only filled with saline solution [Weidler and Diecke, 1969; the exact composition of the ion concentrations is the following: NaCl (178.54 mM; 10.43 g/1000 ml), KCl (17.61 mM; 1.31 g/1000 ml), CaCl2 (7.51 mM; 1.10 g/1000 ml), $MgCl_2$ (25 mM; 5.08 g/1000 ml), HEPES (10 mM; 2.383 g/1000 ml)]. Pilocarpine, a muscarinic agonist of acetylcholine, was used to induce rhythmic activity in thoraco-coxal MNs in the three segmental ganglia (Büschges et al., 1995). In order to achieve long-lasting activity of the CPGs in the three thoracic ganglia, pilocarpine was used at concentrations of 5 mM for the mesothoracic and metathoracic ganglia and of 7 mM for the prothoracic ganglion. The activity of the coxal protractor and retractor MNs was recorded with extracellular hook electrodes from the nervus lateralis 2 (nl2) and nervus lateralis 5 (nl5), respectively (Schmitz et al., 1991). Stepping activity of the respective leg was monitored by electromyograms (EMGs) of the tibial flexor muscle, which is active during stance phase. In these recordings, two copper wires (40 µm) were used (Gabriel et al., 2003). Extracellularly recorded MN activity and EMGs were amplified (500–5000×, depending on the recording quality) and filtered (300 Hz to 3 kHz for extracellular recordings, 50 Hz to 1 kHz for EMGs). Subsequently, the recordings were digitalized by a MICRO 1401 A/D converter (sampling rate: 12.5 kHz, Cambridge Electronic Design). For recordings, SPIKE2 data analysis software (version 5.21, Cambridge Electronic Design) was used. To improve the analysis of noisy data, the extracellular recordings were rectified and smoothed using time constants from the range [0.008,0.08] s. The output at time t is the average value of the input data points in the time interval $[t-\tau, t+\tau]$ s, τ being the time constant as computed by the smoothing function of SPIKE2.

In the experiments, we studied two kinds of leg movements. First, the intact leg was positioned on the treadmill and the treadmill was moved either manually or motor operated by a custom-written stimulation program in SPIKE2. The movement of the treadmill resulted in passive displacements of the stick insect leg, which we denoted as "enforced stance phases." The movement of the treadmill was monitored by a tachometer. Second, the intact leg performed self-generated, active steps on a low friction treadmill positioned parallel to the body axis of the animal (Gabriel et al., 2003). This stepping movement approximately mimics the kinematics during straight forward and backward walking of stick insects (Gabriel et al., 2003). A positive amplitude in the tachometer trace represents the stance phase of a forward step (Borgmann et al., 2009), or more precisely the backward movement of the leg relative to the body. In this case, we observed a caudally directed movement of the treadmill. A negative amplitude represents the stance phase of a backward step, or the tarsal movement of the leg reflecting a backward step. In this case, we observed a rostrally directed movement of the treadmill. The maximum or minimum amplitude of the velocity signal represents the end of a stance phase. In all experiments the animal performed an active swing phase to complete a full step, whereas the stance phase was either active or passive, i.e., enforced. Depending on the stepping direction the retractor muscle (forward step) or the protractor muscle (backward step) was active during the stance phase.

In our experiments, we had to exclude a possible central effect of the pilocarpine-induced rhythmic activity of the thoracic protractor-retractor CPG on other thoracic ganglia that were not affected by pilocarpine. A central effect would mean that the pharmacologically induced rhythm of the protractor and retractor CPGs would lead to further, possibly rhythmic, activity in the adjacent ganglia. To this end, we used a split

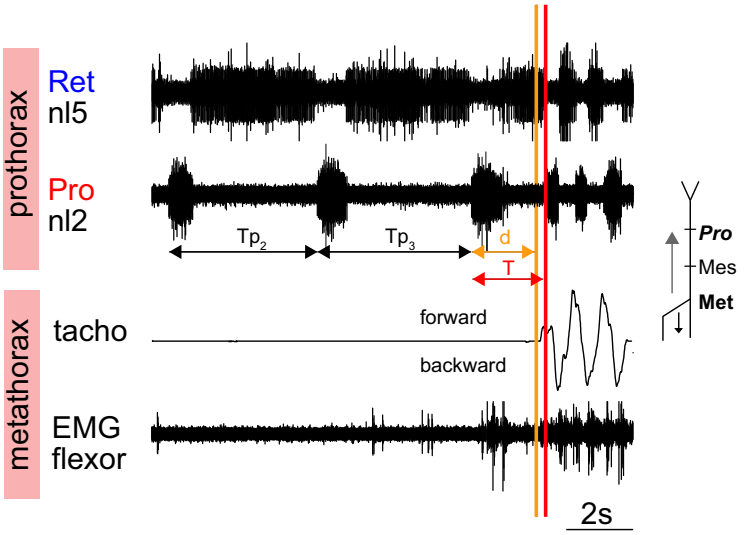

Figure 1. Example for data point extraction and analysis. The two upper traces show extracellularly recorded activity of the retractor (nl5) and protractor (nl2) MNs of the prothoracic ganglion under the influence of pilocarpine. The two lower traces display the treadmill movements (tacho), and the activity (EMG) of the flexor muscle of the ipsilateral hind leg. The periods of the cyclic activity of the protractor MNs Tp_1, Tp_2, and Tp_3 (of which only Tp_2 and Tp_3 are shown; black, two-headed arrows) are averaged to obtain the mean period T_p (not shown in the figure). These cycles immediately precede the next stance phase whose start is marked by an orange vertical line. Hence, *d* (orange, two-headed arrow) is the time from the start of the last protractor MN burst to the start of this stance phase. Finally, *T* (red, two-headed arrow) denotes the time from the start of the last protractor MN burst before this stance phase to the start of the next protractor MN burst (red vertical line). The schematic of a stick insect on the right-hand side illustrates the experimental arrangement: the hind leg of the metathoracic segment (bold) performs a forward stance phase (black arrow), and the effect of this action on the activity of the protractor and retractor MNs of the prothoracic ganglion (bold italic) is analyzed (gray arrow).

bath preparation as described above for the ganglion where pilocarpine solution was applied. In this experimental arrangement, all lateral nerves were cut, and the nerves whose activity was recorded were crushed distally to the recording site to remove any signals from the periphery. We then recorded the activity of the protractor and retractor MNs of all ganglia by means of extracellular hook electrodes continuously before and after pilocarpine application.

In order to investigate the source of sensory signals, deriving from the animals' ipsilateral hind legs, that contribute to the entrainment of the prothoracic CPG activity, an additional experimental condition was introduced. The aim was to stimulate in an isolated way the femoral and trochanteral campaniform sensilla (f/tCS). For this purpose, the left hind leg was amputated at the femur-tibia joint. The coxa-trochanter joint was then fixed by dental cement (PROTEMP II, ESPE) to block movement of this joint. Flexor activity was recorded as reported for the intact leg preparation. Afterwards, the stump was slightly bent manually in a backward direction until a flexor activation was detectable, parallel to the stick insect's body resulting in load signals that could be detected by the f/tCS (Schmitz, 1993). The rest of the preparation was prepared as described before for the intact leg preparation.

Data analysis and statistics

We analyzed the transitions between the protractor and retractor MN burst activities when the hind leg was stepping in four experimental conditions: active and enforced forward stepping and active and enforced backward stepping. The steps were counted and for the statistical analysis weighted for all animals. Not all animals had the same number of steps or stepping sequences. In order to achieve a balanced and nonbiased result we calculated the weight of each animals' contribution to the step count by using the formular W (weight) = T (target proportion)/A (actual sample proportion). We calculated the mean and SEMs. The occurrences of the different transitions during stepping were compared, and tested for significance (significance levels: $^{*}p < 0.05$, $^{**}p < 0.01$, $^{***}p < 0.001$) using the Wilcoxon rank sum test for paired comparison and the Kruskal–Wallis test for the multicomparison for nonparametric data as well as a Dunn's test for the correction for multiple comparisons as implemented in MATLAB [version: R2011b (7.13.0.564); The MathWorks]. Phase histograms as well as cross-correlation analysis were conducted using the SPIKE2 analysis software to compare the relative onset occurrence of the protractor and retractor bursts within a step cycle and the correlation of the protractor and retractor MN rhythms in the different segments. The experimental data were imported into MATLAB, and the significance of these correlations was tested by the Pearson's correlation test with the rectified and smoothed traces (τ = 0.08) at a time lag of $t = 0$ s. Circular statistics for the spike distributions of a step cycle in the unit circle were performed using the circular statistics toolbox of MATLAB (Berens, 2009). The Rayleigh test (Batschelet, 1981) was used to test whether spikes of the protractor and retractor MN activity were randomly distributed, or whether a predominant directionality was present. To analyze the effect of the enforced steps of the different legs on the pilocarpine-induced protractor and retractor MN rhythm in the other two thoracic ganglia, phase response curves (PRCs) were calculated using the following formula:

$$\left(\frac{d}{\overline{Tp}}\right) = \frac{\overline{Tp} - T}{\overline{Tp}}.$$

Figure 1 illustrates the parameters used for the calculation of the PRC. T_p represents the mean duration of three consecutive protractor MN cycles (two of which are shown in Fig. 1, Tp_2 and Tp_3) before the start of a stance phase (Fig. 1, orange line). *T* (Fig. 1, red) is the duration between two protractor MN bursts. In our example in Figure 1 this is the last (pilocarpine-induced) protractor MN burst (nl2) before the onset of a stance phase of the ipsilateral hind leg until the start of the first pilocarpine-induced protractor MN burst immediately after the onset of a stance phase of the ipsilateral hind leg (orange line); *d* (Fig. 1, orange) is the time between the start of the last pilocarpine-induced protractor MN burst before a step and the start of a stance phase of the ipsilateral leg (orange line). In the text and in the figures, *N* is the number of animals and *n* is the total number of step cycles for all animals. All tests, number of experimental animals, repetitions and significances are listed in the figure captions.

Results

Artificially enforced stepping of the hind leg entrains pilocarpine-induced rhythmic activity in prothoracic protractor and retractor MNs

To investigate the existence of a long range caudo-rostral sensory influence between the metathoracic and prothoracic ganglion of a stick insect, we made use of a so-called split-bath preparation, where the isolated prothoracic ganglion was exposed and under pharmacological influence of 7 mM pilocarpine, and the left hind leg was intact and stepping on a treadmill (see Materials and Methods). To exclude any central influence on the central pattern generating networks of the metathoracic ganglion, we decided to enforce artificial forward stepping of the hind leg, as it does not require an activation of the leg muscles in the first place. This allowed us to elicit sensory information posteriorly, hence allowing us to study the direction the posterior-anterior traveling sensory information might have on activated prothoracic CPGs. We therefore moved the respective leg by moving the treadmill and thereby enforced passive leg movements that, to some extent, reflected the kinematics of a leg during stance phase. When moving the treadmill, and hence enforcing a stance phase,

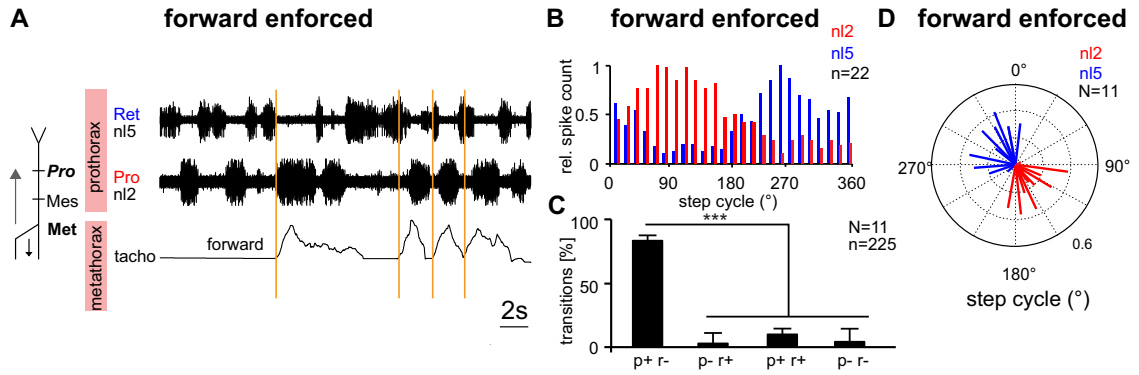

Figure 2. Enforced forward stepping of the ipsilateral hind leg entrains pilocarpine-induced rhythmic activity of the prothoracic protractor and retractor CPG. ***A***, Extracellular recordings from protractor MNs (nl2) and retractor MNs (nl5) in the prothoracic ganglion, as indicated; tachometer signal of the treadmill. A positive amplitude in the tacho trace represents a stance phase during a forward step. Protractor MN activity is coupled to the stance phase of enforced forward steps of the hind leg (orange lines). ***B***, Phase histogram showing the relative spike counts in the protractor (red) and retractor (blue) MN discharges within an enforced forward step cycle in one animal. ***C***, Relative proportion of the transitions between MN activities at the start of an enforced hind leg stance phase for forward stepping. p+r– = start of protractor activity and end of retractor activity. p–r+ = end of protractor activity and start of retractor activity. p+r+ = co-activation of both MN pools. p–r– = no MN activity observed after the start of a hind leg stance phase ($N = 11$). Pairwise comparisons were performed with the Wilcoxon rank-sum test and multiple comparisons using the Kruskal–Wallis test with a Dunn's correction for multiple comparisons, $^{***}p < 0.001$, error bars = SEMs. ***D***, Prothoracic protractor and retractor MN burst activity during enforced forward stance phases of the hind leg ($N = 11$). Circular plot shows mean vectors of nl2 (red) and nl5 (blue) MN activity within a step cycle (Rayleigh test for circular data, $p < 0.001$). N = number of animals, n = number of steps.

the animals actively completed the step cycle by performing the swing phase voluntarily. Figure 2*A* shows an example for these enforced forward steps. The stance phases of the forced forward steps of the hind leg evoked simultaneous prothoracic protractor MN activity and were able to entrain the pilocarpine-induced rhythm (Fig. 2*A*, orange lines). The phase histogram for the enforced forward steps in Figure 2*B* shows a distribution of prothoracic MN activity within a stepping cycle of the hind leg for one animal. The prothoracic protractor MNs (red) attain their maximal spike count during the stance phase (0−270°), the prothoracic retractor MNs (blue) during the swing phase (270−360°). We defined the prothoracic protractor MN burst onset that was observed during ground contact of the enforced movement of the hind leg as the transition from retractor MNs being active and protractor MNs being quiescent to retractor MNs being quiescent and protractor MNs being active. Because of the alternating nature of the MN activity, the protractor MNs in the prothoracic ganglion were released from their inhibition and hence showed an increase in firing rate, which we denoted by p+ (Schmidt et al., 2001; Rosenbaum et al., 2015). This increased protractor MN activity coincided with a cessation of prothoracic retractor MN activity, denoted by r–. Thus, the transition became (p+r–). Three other transitions could be defined in a similar way (Fig. 2*C*). Figure 2*C* shows the average relative occurrence of these transitions in all animals. A transition of p+r– indicates a potential onset of a swing phase of the ipsilateral leg. Behaviorally, this would be an indicator of the start of a metachronal wave (Grabowska et al., 2012), and in agreement with established coordination rules in terrestrial insect locomotion (Cruse, 1990). Transitions evoked by the enforced forward steps of the hind leg produced p+r– transitions in 83.6%, which was significantly higher than any other transition ($N = 11$, $n = 225$ steps, $p < 0.001$, Kruskal–Wallis test; Fig. 2*C*). For the enforced steps, the alternating bursting, and the distribution of the MN spikes within a step cycle of the hind leg for both MN pools, as seen in a typical example from one animal in Figure 2*B*, are similar for ten other animals (see Fig. 2*D*). The mean vectors of the distributions of MN activity during a step cycle of the hind leg for each animal (one vector per animal, minimum 5 steps included) showed a clear opposite directionality between "protractor" (red) and "retractor" (blue) vectors. All ($N = 10$) but one mean "retractor" vector in one animal show significant directionality. The range of angular coordinates of the mean vectors was [94°,196°] for the "protractor" vectors, and [246°,8°] for the "retractor" ones [$N = 11$, $p < 0.001$ (Rayleigh test), except for one case of nl5 activity; Fig. 2*D*].

The effect of enforced hind leg stepping on the mesothoracic CPGs

Our results so far do not provide information about the activity of the mesothoracic ganglion during enforced leg movements of the hind leg, as we specifically only activated the prothoracic ganglion pharmacologically. Previous work has shown that hind leg forward stepping was accompanied by a general increase in mesothoracic protractor and retractor MN activity (Borgmann et al., 2007). To test whether artificially enforced hind leg steps have the same influence on the mesothoracic protractor-retractor CPG as on the prothoracic one, simultaneous recordings from the protractor and retractor MNs of the prothoracic and mesothoracic ganglion, both under the influence of pilocarpine (prothorax: 7 mM pilocarpine solution and mesothorax: 5 mM pilocarpine solution), were performed. We analyzed the effect of an artificially enforced stance phase of the ipsilateral hind leg on the pilocarpine-induced rhythms by means of cross-correlation analysis of the activities of their MNs. We took three prothoracic protractor MN cycles as reference cycles for the cross correlations. Figure 3*A* shows how a forward stepping ipsilateral hind leg entrained the pilocarpine-induced rhythms of the prothoracic and mesothoracic protractor MNs. With no hind leg stance phases being performed, both pilocarpine rhythms were uncorrelated (Fig. 3*A*, left correlation diagram, $p > 0.05$, Pearson's correlation test, $r^2 = 0.27$). During the three enforced hind leg stance phases, indicated by the orange lines in Figure 3*A*, both rhythms were positively correlated with a correlation coefficient of 0.68 (Fig. 3*A*, middle correlation diagram, $p < 0.001$, Pearson's correlation test). Immediately after stepping, the activities of the pilocarpine-induced nl2 rhythms remained correlated at a time lag of $t = 1$ s (Fig. 3*A*, right correlation diagram, $p < 0.05$, Pearson's correlation test, $r^2 = 0.41$). In both thoracic ganglia, the enforced forward step evoked correlated activity of the protractor MNs. This experiment was performed

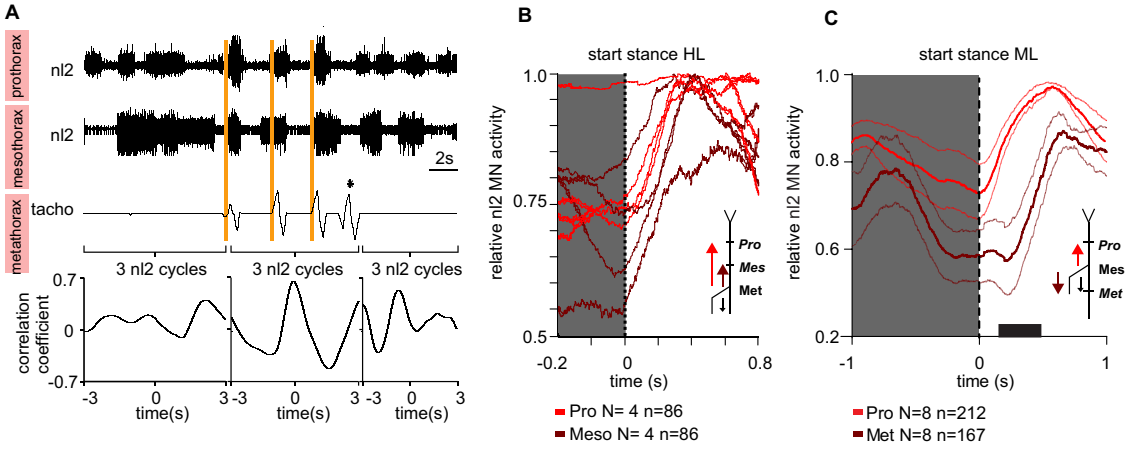

Figure 3. Ipsilateral hind leg stepping entrains the pilocarpine-induced rhythmic activity of the prothoracic and mesothoracic protractor and retractor CPGs. ***A***, Upper panel, Extracellular recordings from protractor MNs in the prothoracic and mesothoracic ganglion, as indicated; tachometer signal of the treadmill. Orange vertical lines mark the start of the enforced stance phases. The peak in the tacho trace, marked by a star, led to no protractor MN activation since this stance phase might have occurred too soon within the step cycle of the prothoracic and mesothoracic protractor MNs rhythm. Bottom panel, Cross-correlation function between the two neuronal activities computed before, during and after the induction of the stance phases for a period of 6 s each (Pearson's correlation test). ***B***, Waveform average of prothoracic and mesothoracic protractor MN burst activity after enforced stance phases ($n = 86$, $N = 4$). The diagram shows the reaction time of the prothoracic (light red) and mesothoracic (dark red) protractor MNs after an enforced forward stance phase of the hind leg ($t = 0$). The schematic of a stick insect indicates the experimental setup. The large light red and dark red arrows show the direction of influence of the stepping hind leg to be investigated, the small black arrow the direction of the leg movement during the enforced stance phase. ***C***, Forward walking of the middle leg results in a faster nl2 activity onset in the prothoracic ganglion than in the metathoracic ganglion. Waveform average of relative nl2 MN activity of prothoracic (light red) and metathoracic (dark red) protractor MN burst activity after stance phase enforcements [$n = 167$ (metathorax); $n = 212$ (prothorax), $N = 8$]. Significance in onset difference is shown as black bar on the x-axis with $p < 0.05$. Faded lines display SEMs. Differences in the curves were calculated using multiple paired t tests per time point and correcting for false discovery rate (FDR) using the two-stage step-up method previously described (Benjamini et al., 2006) with a FDR = 1%. The schematic of a stick insect indicates the experimental setup. The large dark red and light red arrows show the direction of influence of the stepping hind leg to be investigated, the small black arrow the direction of the leg movement during the enforced stance phase. N = number of animals, n = number of steps.

on three additional animals, yielding similar results. Figure 3*B* displays the waveform average of the protractor MN activity ($N = 4$) in the prothoracic ganglion (light red), and the mesothoracic ganglion (dark red) after the start of a forward stance phase of the hind leg ($n = 86$ steps). In all cases, except for one animal (steady tonic activity of prothoracic protractor MNs), the activities of the protractor MNs emerged between 0 and 0.4 s after the start of the stance phase and were positively correlated with a peak at $t = 0$ [$p < 0.01$, Pearson's correlation test, $r^2 = 0.74$; correlation calculated on average of all animals ($N = 3$) after excluding the animal that was only displaying tonic nl2 MN activity].

Our study indicates that a stepping hind leg entrains the active prothoracic protractor-retractor CPG because of afferent sensory signals, such as loading signals. In our first set of experiments as shown in Figure 2, where we do not pharmacologically activate the mesothoracic ganglion (see Materials and Methods), we show that the mesothoracic protractor-retractor CPG does not have to be activated to transmit the sensory information of a stepping hind leg to the prothoracic protractor-retractor CPG. We furthermore observe that the mesothoracic ganglion is entrained the same way as the prothoracic ganglion when its thoracic CPGs are pharmacologically activated (Fig. 3*A*,*B*).

Artificially enforced stepping of one leg has the same effect on the pilocarpine-induced rhythmic activity of the protractor and retractor MNs in all other thoracic ganglia

Previous studies showed that a spontaneously walking front leg activates CPGs in the mesothoracic ganglion and induces tonic MN activity in the metathoracic ganglion (Borgmann et al., 2009). As we do not study active walking steps, but rather enforce stepping by moving the legs in a backward direction, we mostly can exclude a central activation of the thoracic CPGs. Our findings so far indicate no hierarchical differences in the entraining influence of the sensory signals coming from a stepping leg. We tested whether this applied to entraining influences of any stepping leg and all pharmacologically-activated, thoracic, protractor-retractor CPGs. As in our previous experiments, we used enforced steps to ensure a better control over step frequency and duration and also to exclude central influences.

Figure 3*C* shows the effect of an enforced forward step of the middle leg on the activity of the prothoracic and metathoracic protractor MNs, which were activated by a 7 and 5 mM pilocarpine solution, respectively. The mean onset of prothoracic nl2 MN activity following a step initiation by the ipsilateral middle leg was significantly faster compared with the onset of the metathoracic nl2 MN activity (black bar on x-axis in Fig. 3*C*, $p < 0.05$). Interestingly, this difference was not found when we analyzed the influence of a stepping hind leg on the ipsilateral prothoracic and mesothoracic nl2 MNs (Fig. 3*B*). In general, the activity of the protractor MNs of both the prothoracic and metathoracic ganglion was still positively correlated with the start of the enforced stance phase of the stepping middle leg in 8 out of 8 experiments ($n = 167$ cycles, $p < 0.0001$, Pearson's correlation test, $r^2 = 0.8185$) for the metathoracic ganglion and in six out of eight experiments ($n = 212$ cycles, $p < 0.0001$, Pearson's correlation test, $r^2 = 0.2543$) for the prothoracic ganglion (Fig. 3*C*).

For further characterization of the effects an enforced stepping of a leg has on the pilocarpine-activated protractor-retractor CPGs of the other two segments, we calculated the PRCs for all possible experimental conditions (Fig. 4). It is noteworthy that all experimental situations led to very similar results. Regardless of the leg and the direction of the sensory signal flow, an enforced forward step was always followed by the activation of the protractor MNs in the other two hemisegments (Pearson's correlation, $p < 0.01$ for all cases, except for the case "HL on mesothorax" in Fig. 4, where $p < 0.05$).

Finally, we analyzed every enforced forward step of every stepping leg for all animals. We calculated the proportion of the successful entrainments, i.e., when the stepping entrained the pilocarpine-induced rhythms in any of the other two thoracic ganglia. The results were weighted by taking into account the overall step number for each animal and compared using the Wilcoxon rank-sum test for paired comparisons and the Kruskal–Wallis test for multiple comparisons. Table 1 shows that in all experimental conditions, an enforced forward step evoked an entrainment of the protractor-retractor CPG in the other two ganglia. These results were significant at $p < 0.001$.

Our findings therefore clearly show that the entrainment of the MN activity in one segment, evoked by sensory pathways activated during steps of a leg in a different segment, is a universal property of the stick insect's neuro-mechanical system. However, it can only be discerned if the segmental CPGs have already been periodically active before the leg starts stepping, potentially indicating a state-dependent entrainment.

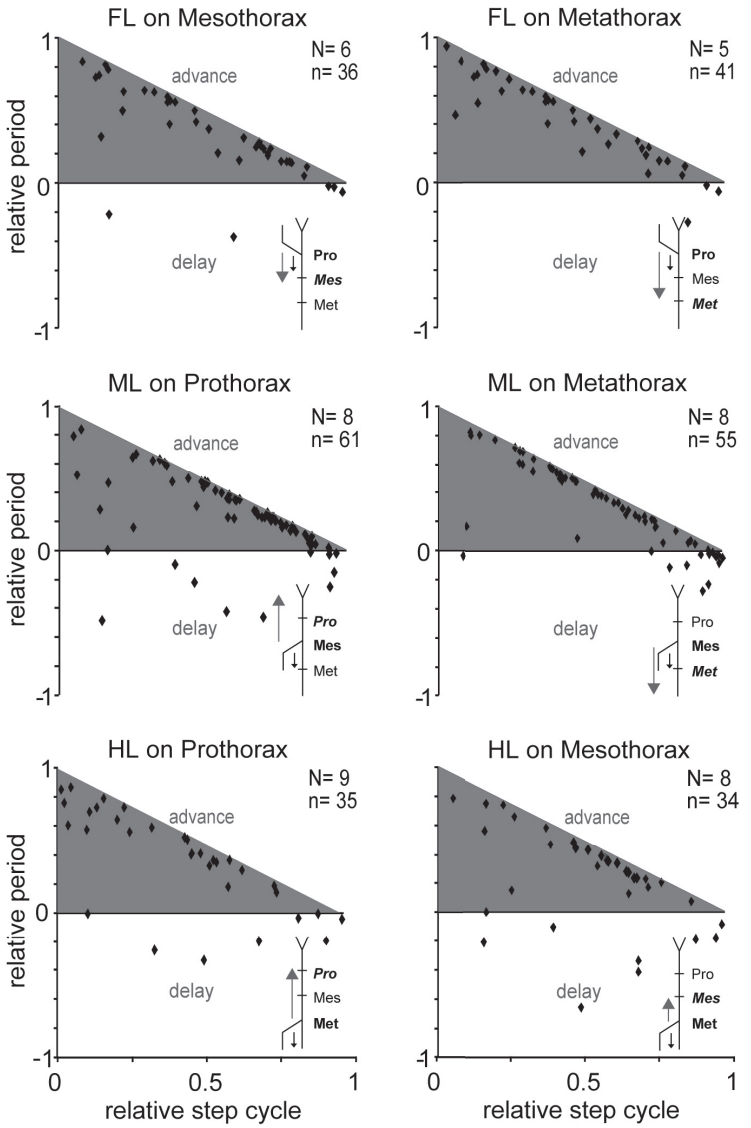

Figure 4. Relation between enforced forward leg movements and protractor MN burst activity in the other two deafferented thoracic ganglia activated by pilocarpine. The panels show PRCs. Upper panels, Front leg (FL) forward stance phases triggered entrainment of the rhythmic activity of the MNs of the two other segments: correlation coefficient $c = -0.99$ and $p < 0.001$ for the mesothoracic, and $c = -0.69$ and $p < 0.001$ for the metathoracic ganglion. Middle panels, Middle leg (ML) stance phases triggered entrainment of the rhythmic MN activity in the adjacent ganglia with $c = -0.61$ and $p < 0.001$ in the prothoracic, and $c = -0.8347$ and $p < 0.001$ in the metathoracic ganglion. Bottom panels, Hind leg (HL) stance phases triggered entrainment of the rhythmic activity of the prothoracic and mesothoracic protractor MNs with $c = -0.76$ and $p < 0.001$ and $c = -0.46$ and $p < 0.05$ (0.037), respectively. The schematic of a stick insect below each individual panel indicates the experimental arrangement in each condition. Segment names written in bold denote the segment of the leg movement, whereas segment names in bold italic the segments under the influence of pilocarpine. The large gray arrow shows the direction of influence of the stepping leg to be investigated, while the small black arrow shows the direction of the stance phase (forward steps for all situations shown).

Entrainment of the pilocarpine-induced rhythm in the prothoracic protractor and retractor MNs by enforced backward stepping of a hind leg

Since different neurons in the same and adjacent thoracic segments are activated (Rosenbaum et al., 2010, 2015) during the stance phases of forward and backward steps we tested whether an enforced backward stepping hind leg has similar entrainment properties on the pharmacologically activated prothoracic ganglion as an enforced forward stepping hind leg. Our results are shown in Figure 5. Enforced stance phases of a backward stepping hind leg evoked prothoracic retractor activity (Fig. 5*A*). During 20 enforced backward steps in one animal, the prothoracic retractor MNs (blue) were, on average, active during the stance phase, whereas the prothoracic protractor MNs (red) were active during the swing phase (Fig. 5*B*). Enforced backward steps ($N = 11$, $n = 225$ steps) evoked an activation of prothoracic retractor MNs and a cessation of prothoracic protractor MNs (Fig. 5*C*) in on average 69.8% of the enforced backward steps (***$p < 0.001$ and **$p < 0.01$ compared with other transitions, Kruskal–Wallis test). The circular plot in Figure 5*D* illustrates the distributions for the enforced backward steps of the hind leg. For enforced backward steps, except for two animals out of the 11 tested animals, the activity of the two MN pools alternated, with a significant directional preference ($p < 0.001$, Rayleigh test) within the step cycle of a single, stepping hind leg. The ranges of angular coordinates were [279°,89°] for the protractor and [71°,210°] for the retractor vectors.

These results show that the entraining long-range influence from the stepping hind leg to the prothoracic ganglion is dependent of the stepping direction.

Active forward and backward stepping of the hind leg leads to entrainment of pilocarpine-induced rhythm in the prothoracic protractor and retractor CPGs

To exclude entrainment and activation effects of CPGs that may arise because of active, voluntarily induced steps by the stick insects, we applied a method where we enforced the leg

Table 1. Summary of all enforced forward stance phases and the resulting entrainment of the pilocarpine-induced rhythm in the remaining ganglia for all animals tested

	Prothorax	Mesothorax	Metathorax
Forward steps of			
FL	—	$N = 9$ (84%)	$N = 6$ (81%)
ML	$N = 9$ (83%)	—	$N = 9$ (87.5%)
HL	$N = 17$ (84.5%)	$N = 6$ (82.6%)	—

The rows show the leg that does the stepping, the columns are the thoracic segments (ganglia) that are affected by the stepping leg. In the table panels, the percentage is the proportion of successful entrainments and N is the number of animals used. These results were obtained with the pairwise Wilcoxon rank-sum test. Note that all of them indicate significant entrainment ($p < 0.001$).

movements. In this way we could control for regularity, sensory signals, and duration of a step. Nevertheless, because of the different nature of step initiation, these enforced movements could result in different sensory inputs (different load or direction signals) to the neighboring CPG networks than active steps would do. Further, the activation of protractor-retractor CPGs by voluntary steps of the hind leg could have a different effect on pharmacologically activated prothoracic CPG activity. To compare the entraining properties of active and enforced stepping we performed experiments where the animal was stepping actively forward and backward with its hind leg.

A backward stepping hind leg entrained the activity of prothoracic protractor and retractor MNs (Fig. 6*A*, orange lines). During the stance phase (0−270° of the step cycle) of a self-generated backward step of the ipsilateral hind leg, the prothoracic retractor MNs (blue) showed the maximal spike count, which was alternating with the maximal spike count of the prothoracic protractor MNs (red) in the swing phase (270−360° of the step cycle) of the stepping hind leg (Fig. 6*B*, a typical example from one animal). This is also visible in the relative frequency of occurrence of the transitions (Fig. 6*C*, $N = 9$). The start of a backward stance phase is followed by the onset of prothoracic retractor MN activity, and the end of the activity of the prothoracic protractor MNs (transition p–r+) on average in 56.5%, which is significantly different from all other transitions [p+r–, p–r– ($p < 0.001$), and p+r+ ($p < 0.01$), Kruskal–Wallis test]. The spike distribution of the protractor and retractor MNs within a step cycle was similar for all animals tested. The circular plot in Figure 6*D* illustrates these distributions for active backward stepping of these nine animals. The prothoracic protractor MN activity was rhythmically alternating with the retractor MN activity in all cases, and the directional preference of the distributions expressed by the mean vector length was significant at a level of $p < 0.001$ for all cases, except for one distribution of prothoracic protractor MN activity in one animal (Rayleigh test). The angular ranges were [294°,10°] for "protractor," and [58°,188°] for "retractor" vectors.

Tethered stick insects do not prefer forward walking when all legs, except the hind legs are removed. We nevertheless could observe four animals performing active forward steps with the hind legs. We observed that when the CPGs in the prothoracic ganglion are activated by pilocarpine in an experimental split-bath, the forward stepping hind leg entrained the activity of the prothoracic MNs (Fig. 6*E*, orange lines). The distribution of the number of spikes of the prothoracic retractor (blue) and protractor (red) MNs within one step cycle of the hind leg showed the alternating activity of the MN pools (Fig. 6*F*, a typical example from one animal). During the stance phase, which is approximately the range [0°,270°] of a step cycle, the prothoracic protractor MNs showed the maximal spike count, whereas the retractor MNs showed an increase in the spike count at the beginning and during the swing phase [270°,360°]. Figure 6*G* shows the relative occurrence of these transitions, where a transition of p+r– indicates a potential onset of a swing phase. Behaviorally, this would be an indicator of the start of a metachronal wave (Grabowska et al., 2012), and in agreement with established coordination rules in terrestrial insect locomotion (Cruse, 1990). A forward stepping hind leg evoked activation of prothoracic protractor MNs, which in turn lead to a quiescence of prothoracic retractor MNs on average in 65.2% of all cases ($N = 4$, $n = 23$), which was significantly higher than any other observed transition ($p < 0.001$, Kruskal–Wallis test). The entrainment of the prothoracic protractor MNs by the stepping hind leg occurred altogether in all three animals that spontaneously walked forward with their hind leg (Fig. 6*H*). The mean vectors of the distributions of MN activity during a step cycle for each animal ($N = 3$, one vector per animal, minimum 5 steps included; one animal had to be excluded, because of too few steps) showed, except for one case, significant directional preferences at a level of $p < 0.001$ (Rayleigh test). The mean values of the angular coordinates of the vectors of protractor MN activity within a hind leg step cycle are between 343.8° and 118.2°, for retractor MN activity the angular range is from 170.8° to 335.7°.

Our results show that for the entrainment of pilocarpine-induced rhythms, it is irrelevant whether the leg performs an active or artificially enforced stance phase, excluding an exclusive central influence in the generation of ipsilateral leg coordination.

Nonspecific stimulation of f/tCS by backward bending of the hind leg stump entrains the pilocarpine induced rhythm in the prothoracic protractor-retractor CPG

Next, we were determined to identify the source of the sensory information that arises at the stepping hind leg and entrains the pilocarpine-induced rhythm in the prothoracic protractor-retractor CPG. For these experiments, the hind leg was fixed at the coxa-trochanter joint to immobilize it. To exclude ground contact, and sensory information arising from the chordotonal organ, the leg was cut in the middle of the femur (see Materials and Methods; Fig. 7*A*, upper panel). The leg stump was then slowly bent in a backward direction, mimicking loading signals that are encoded by the campaniform sensilla of the stick insect (Akay et al., 2004). Figure 7 shows the results of these experiments. Bending the leg in a backward direction resulted in flexor activation of the hind leg and entrainment of pharmacologically induced prothoracic protractor and retractor CPG activity (Fig. 7*A*). The protractor burst onsets (red lines) were observed directly after leg stump movement (green lines), resulting in an advancement of the pilocarpine-induced rhythm, i.e., a shortening of its period, in response to every stimulus (Fig. 7*B*, $n = 14$). This result is comparable to the PRCs given in Figure 4 in which the effect of enforced leg stepping on the pilocarpine-activated protractor and retractor CPGs of neighboring segments is shown.

Our results conclude that the sensory signals, entraining the prothoracic protractor-retractor CPG, could derive from load signals detected by the campaniform sensilla, which are sufficient to evoke a similar prothoracic protractor-retractor entrainment as observed in the intact leg preparations.

Discussion

In this work, we provide experimental evidence for a caudo-rostral effect driven by peripheral sensory signals deriving from the

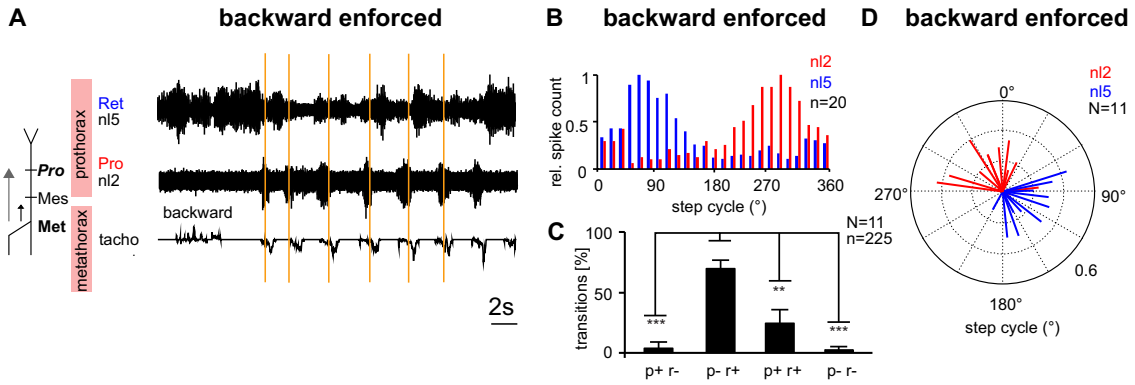

Figure 5. An enforced backwards stance phase results in the entrainment of the pilocarpine-induced rhythmic activity of the prothoracic protractor and retractor CPG. ***A***, Extracellular recordings from protractor MNs (nl2) and retractor MNs (nl5) in the prothoracic ganglion, as indicated; tachometer signal of the treadmill. A negative amplitude in the tacho trace represents a stance phase during a backward step. The onsets of the backward stance phases (orange vertical lines) are immediately followed by prothoracic retractor activity and protractor quiescence. ***B***, Phase histogram showing the relative spike counts in the protractor (red) and retractor (blue) MN discharges within an enforced backward step cycle. This phase histogram was obtained over 20 steps in one animal. ***C***, Proportions of transitions during a step cycle of an enforced backwards moved hind leg (abbreviations are the same as in Fig. 2*C*). Pairwise comparisons were performed with the Wilcoxon rank-sum test and multiple comparisons using the Kruskal–Wallis test with a Dunn's correction for multiple comparisons; $^{**}p < 0.01$, $^{***}p < 0.001$, error bars = SEMs. ***D***, Mean vectors of the prothoracic protractor and retractor MN spike distribution during enforced backward stepping ($N = 11$). All except two mean vectors of the prothoracic protractor and retractor MN activity show significant directionality (Rayleigh test for circular data, $p < 0.001$). N = number of animals, n = number of steps.

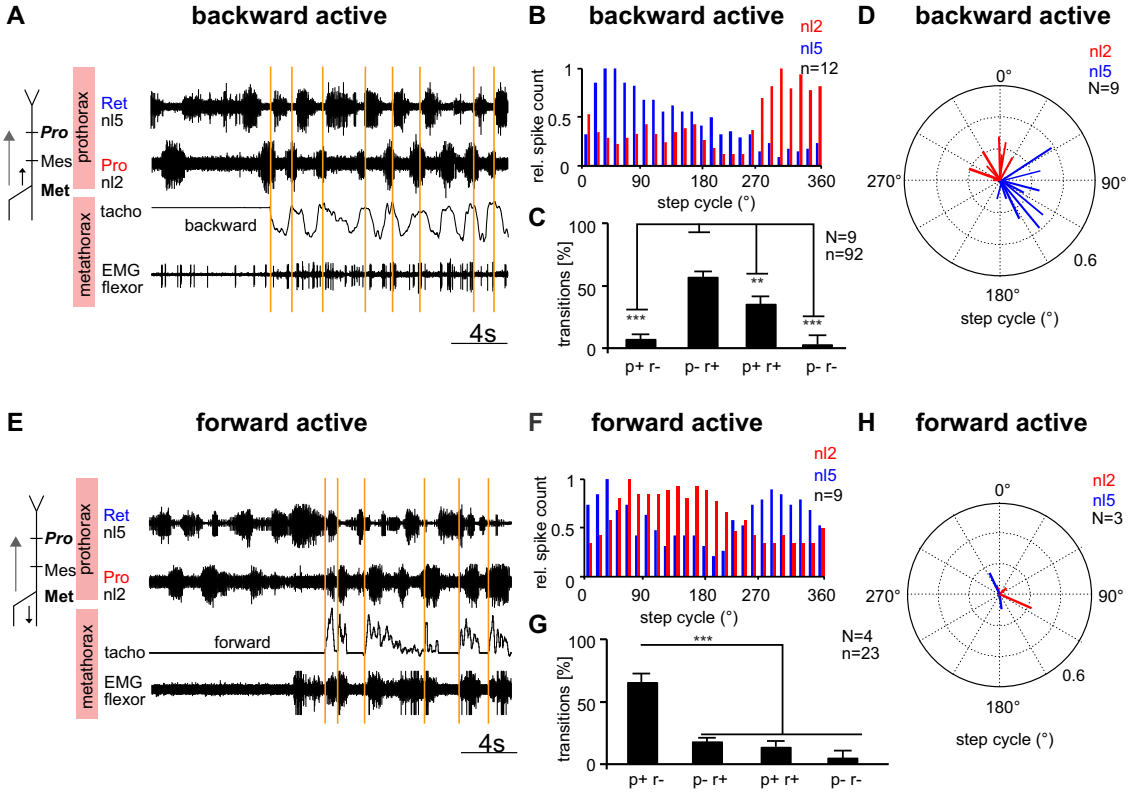

Figure 6. Active stepping of the hind leg in both directions has the same influence on the pilocarpine-induced prothoracic protractor-retractor CPG activity than enforced stepping. ***A***, Retractor MN activity is coupled to the stance phase of self-generated backward steps of the hind leg. Extracellular recordings from protractor MNs (nl2) and retractor MNs (nl5) in the prothoracic ganglion, as indicated; tachometer signal of the treadmill. A negative amplitude in the tacho trace represents a stance phase during a backward step. The beginning of a stance phase is marked by a solid orange vertical line. Bottom trace shows flexor EMG activity of the stepping hind leg. ***B***, Relative MN spike count for nl2 MNs (red) and nl5 MNs (blue) for one animal in a walking sequence of $n = 12$ steps. ***C***, Proportions of transitions for all recorded step cycles ($N = 9$, $n = 92$). Notations are the same as in Figure 2*C*. Pairwise comparisons were performed with the Wilcoxon rank-sum test and multiple comparisons using the Kruskal–Wallis test with a Dunn's correction for multiple comparisons; $^{**}p < 0.01$, $^{***}p < 0.001$, error bars = SEMs. ***D***, Mean vectors of the prothoracic protractor and retractor MN spike distribution during active backward stepping, $N = 9$. All mean vectors ($N = 8$) of the prothoracic protractor and retractor MN activity except for one "protractor" ($N = 1$) vector show significant directionality ($p < 0.001$, Rayleigh test for circular data). ***E***, Extracellular protractor MN activity is coupled to the stance phase of self-generated forward steps of the hind leg. Orange vertical lines: start of stance phases. EMG activity shows flexor muscle activity of the hind leg. The positive amplitude of the tacho trace shows the stance phase of the hind leg. ***F***, Distribution of the protractor (red) and retractor (blue) MN activity, represented by the relative MN spike count ($N = 1$, 9 steps). ***G***, Relative proportion of the transitions between MN activities at the start of an active hind leg stance phase during forward stepping. Notations are the same as in ***C***. Pairwise comparisons were performed with the Wilcoxon rank-sum test and multiple comparisons using the Kruskal–Wallis test with a Dunn's correction for multiple comparisons; $^{***}p < 0.001$, error bars = SEMs. ***H***, Mean vectors of the prothoracic protractor (red) and retractor (blue) MN spike distribution during a forward step cycle of the hind leg ($N = 3$). All but one vector show significant directionality at a significance level of $p < 0.01$ (Rayleigh test for circular data). Upper and Lower panels, The small black arrow in the schematic of a stick insect displays the direction of the leg movement during the stance phase. The gray arrow indicates the direction of the sensory influence that is investigated. N = number of animals, n = number of steps.

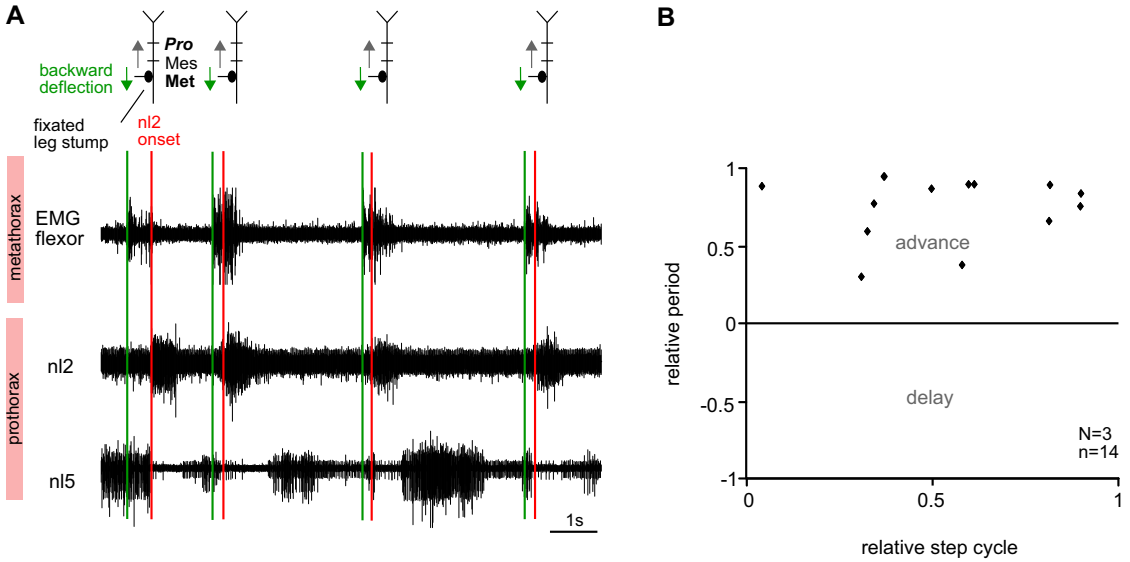

Figure 7. Pilocarpine-induced rhythm in the prothoracic protractor-retractor CPG was entrained by stimulation of campaniform sensilla. ***A***, Upper panel, Scheme of preparation and experimental procedure. The leg was fixated at the coxa-trochanter joint (black) to prevent active movement (see Materials and Methods). The leg stump was then bent (green arrow) in a backward direction mimicking loading signals during a forward step. Lower traces, The flexor muscle of the remaining hind leg stump was activated during bending (green lines). A bending in backward direction resulted in prothoracic protractor (nl2) MN activity (red lines). ***B***, PRC shows that all protractor MN bursts occurred directly after the stimulation (bending). $N = 3$, $n = 14$. N = number of animals, n = number of stimulations.

most caudal metasegment onto prothoracic CPGs in the stick insect *Carausius morosus*. Our experiments show that the activity of f/tCS measuring load in the hind leg was sufficient to evoke an entrainment of pharmacologically activated prothoracic protractor-retractor CPG networks. Furthermore, we show that the effect of a stepping leg on the centrally evoked rhythmic activities in the protractor-retractor CPGs of thoracic ganglia is the same for all stepping legs indicating that there is no hierarchy in the effect of the sensory influences onto activated CPGs of neighboring segments.

Studies have indicated that interneuronal coupling between central pattern generating networks, without adjustments by sensory input, or hardly without, may be sufficient to generate a whole range of more rigid rhythmic activity such as swimming (leech, Cang and Friesen, 2002; lamprey, Grillner, 2006), crawling (leech, Puhl and Mesce, 2008), fast running (Fuchs et al., 2011; David et al., 2016; Grillner and El Manira, 2020), beating of the swimmeret system in crayfish (Smarandache-Wellmann and Grätsch, 2014) or synchrony of beating of the forewings and hindwings in orthopteran flight (for review, see Mantziaris et al., 2020). Such systems, however, cannot replicate slower paced terrestrial locomotion as these forms of rhythmic activity heavily rely on sensory adjustments provoked by the animal's environment and own movements (Sponberg and Full, 2008; Ritzmann and Zill, 2013; Schilling and Cruse, 2020).

Recent research where the CPGs controlling the levator-depressor system of stick insects were rhythmically activated by pilocarpine in all three thoracic ganglia (Mantziaris et al., 2017), showed only a weak coupling between the thoracic CPGs, which did not suffice to reproduce a rhythmicity that is observed during muscle activation in a walking animal. A recent modeling study (Daun et al., 2019), based on these data, investigated putative connections between the aforementioned CPGs using Bayesian model selection (BMS). Models including a direct caudo-rostral coupling from the meta- to the ipsilateral prothoracic ganglion were preferred by BMS to all other coupling structures tested. A different study (Knebel et al., 2017) showed that such a pharmacological activation of the locust metathoracic ganglion leads to coupled activity of the CPGs of the levator-depressor system in the prothoracic and mesothoracic ganglion, indicating a caudo-rostral connectivity within the thoracic CPG network. Such caudo-rostral connections are also known to be present in various other locomotion systems such as the swimmeret system of crayfish (Smarandache-Wellmann and Grätsch, 2014) or lamprey swimming (Grillner, 2006). However, it is still unclear how such a long-range connection would manifest in the physiology of multisegmented, terrestrial insects. Particularly, data about how a walking hind leg in slowly walking insects influences activated CPGs in the prothoracic ganglion have been unavailable until now. Previous work only showed an entrainment of the oscillations of the pharmacologically activated CPGs in the mesothoracic ganglion by a backward stepping hind leg (Borgmann et al., 2007). Meanwhile, mathematical models proposed a long-range caudo-rostral sensory connection representing loading of a leg that proved crucial in generating stable coordination patterns in six-legged walking (Daun-Gruhn and Tóth, 2011; Toth et al., 2015; Tóth and Daun, 2019). Our results verify the existence of this hypothetical connection and thus make an important contribution in understanding neural connectivity in multilegged locomotion.

Interestingly, this effect is dependent on stepping direction: stance phases of hind leg backward steps were able to reset prothoracic protractor-rectractor MN activity mimicking backwards stepping in the opposite way as forward stepping does. This is in agreement with a recent study on stick insect locomotion (Gruhn et al., 2016). There inter-segmental sensory influences deriving from stance phases of stepping legs during turning were shown to be crucial for performing appropriate turns.

Additionally, our findings show that to entrain the pilocarpine-induced rhythm in the prothoracic protractor-retractor system, afferent signals from the mesothoracic ganglion were not necessary. We did not pharmacologically activate the mesothoracic ganglion, excluding thereby a possible entrainment by its activated CPGs, as it has been shown for locusts (Knebel et al., 2017). Hence, we suggest that the sensory

information deriving from the stepping hind leg is transferred by a direct inter-neuronal long-range connection. Previous studies hinted at the putative existence of such connections from the metathoracic to the mesothoracic ganglion in stick insects and locusts (Brunn and Dean, 1994; Burrows, 1996). Even so it is very likely that the leg sensory influences are mediated via ascending interneurons (Büschges, 1989; Laurent and Burrows, 1988), its exact anatomic representation remains to be investigated in the future.

Our results further show that there is a strong similarity of how the front, middle, and hind legs entrain the rhythmic activity of neighboring thoracic CPGs. Once pharmacologically activated, any stepping leg has the same influence on the activated CPGs of the neighboring segments. Thus, sensory information that travels rostro-caudally has the same effect on a pilocarpine-induced rhythm as the one traveling caudo-rostrally. This might be of relevance because of the highly unpredictable terrain these insects usually live in. Hence, the locomotor system of these animals must be highly capable of adaptation to this environment (Schilling and Cruse, 2020). It would not be effective if one leg had a weaker influence on the rest of the locomotor system than another. Our results are different from those of a former study in which the stepping front leg had the capability of generating oscillatory activity in the neighboring mesothoracic segment and increased tonic activity in the protractor-retractor MNs of the metathoracic ganglion (Borgmann et al., 2007). In their study, the authors did not find such behavior when the middle or hind leg was stepping, indicating that movement and locomotion is initiated in the rostral segments.

Despite the similarity between the entraining properties of the leg movements, we did observe a difference in protractor MN activity onset when the middle leg was stepping forward and entraining the pilocarpine-induced rhythms in the prothoracic and metathoracic ganglion (Fig. 3). This is strictly in line with well-established insect coordination rules, according to which the start of a stance phase in the middle leg induces a return stroke (protractor MN activity) in the prothoracic segment, and where caudal positions (end of stance) start a return stroke (protractor MN activity) in the metathoracic segment (Cruse, 1990; Schilling et al., 2013). The difference between prothoracic and metathoracic protractor MNs onset would thus represent a stance period of a forward moving middle leg. Previous behavioral work showed that amputation of the middle legs resulted in highly uncoordinated stepping in freely walking insects, which was not present on amputation of front or hind legs (Grabowska et al., 2012). Borgmann and colleagues (Borgmann et al., 2007) found that a stepping middle leg, although capable of activating prothoracic and metathoracic protractor and retractor MNs, could only induce tonic activity, contrary to the hind and front leg, which were capable of evoking rhythmic activity in MNs of adjacent segments. These studies and our current work highlight the special role that the middle legs play in the walking system of stick insects.

Our results so far indicated that load as a sensory signal measured by an individual leg plays an important role in the entrainment of the rhythmic CPG activity in the neighboring segments. It is known that the sensory signals generated by the f/tCS, which are embedded into the insects' leg cuticle (Delcomyn, 1991; Zill et al., 2010), are sensitive to load and force (Bässler, 1977; Bässler and Büschges, 1998; Akay et al., 2001, 2004). They are most likely different during enforced movements: only movements evoking a resistant force are generating activity in the tCS (Ritzmann and Zill, 2013; Zill et al., 2018). As a result, enforced stance phases most probably supply adjacent segments with sensory input different from that active stance phases would do. Yet, we worked with enforced leg movements to control for regularity and duration of a step and to exclude entrainment and activation of CPGs that may arise because of active steps by the animals. Our comparison between the entrainment of prothoracic MN activity evoked by active and enforced forward and backward stepping of the hind leg suggests that, at least for the protractor-retractor system, differences are negligible. We further show that the stimulation of trochanteral and femoral campaniform sensilla by bending an amputated hind leg stump is sufficient to evoke an entrainment in the ipsilateral pharmacologically activated prothoracic protractor-retractor CPG network. Bending the leg stump in a backward direction resulted in an increase in activity of the prothoracic protractor MNs and a decrease of activity in the retractor MNs. Since we do not activate a specific type of CS, we conclude that for the entrainment of protractor-retractor MN activity in the neighboring segments the loading signal itself can be unspecific. Nevertheless, we do not exclude that this could be the only source of influence. How our results transfer to kinematic situations other than the one investigated here remains to be studied in future work.

References

Akay T, Bässler U, Gerharz P, Büschges A (2001) The role of sensory signals from the insect coxa-trochanteral joint in controlling motor activity of the femur-tibia joint. J Neurophysiol 85:594–604.

Akay T, Haehn S, Schmitz J, Büschges A (2004) Signals from load sensors underlie interjoint coordination during stepping movements of the stick insect leg. J Neurophysiol 92:42–51.

Bässler U (1977) Sense organs in the femur of the stick insect and their relevance to the control of position of the femur-tibia-joint. J Comp Physiol 121:99–113.

Bässler U, Büschges A (1998) Pattern generation for stick insect walking movements—multisensory control of a locomotor program. Brain Res Brain Res Rev 27:65–88.

Batschelet E (1981) Circular statistics in biology. San Diego: Academic Press.

Benjamini Y, Krieger AM, Yekutieli D (2006) Adaptive linear step-up procedures that control the false discovery rate. Biometrika 93:491–507.

Berens P (2009) CircStat: a MATLAB toolbox for circular statistics. J Stat Soft 31. Available at http://www.jstatsoft.org/v31/i10/. Accessed February 8, 2021.

Borgmann A, Scharstein H, Büschges A (2007) Intersegmental coordination: influence of a single walking leg on the neighboring segments in the stick insect walking system. J Neurophysiol 98:1685–1696.

Borgmann A, Hooper SL, Büschges A (2009) Sensory feedback induced by front-leg stepping entrains the activity of central pattern generators in caudal segments of the stick insect walking system. J Neurosci 29:2972–2983.

Brunn DE, Dean J (1994) Intersegmental and local interneurons in the metathorax of the stick insect *Carausius morosus* that monitor middle leg position. J Neurophysiol 72:1208–1219.

Büschges A (1989) Processing of sensory input from the femoral chordotonal organ by spiking interneurones of stick insects. J Exp Biol 144:81–111.

Büschges A, Schmitz J, Bässler U (1995) Rhythmic patterns in the thoracic nerve cord of the stick insect induced by pilocarpine. J Exp Biol 198:435–456.

Burrows M (1996) The neurobiology of an insect brain. Oxford; New York: Oxford University Press.

Cang J, Friesen WO (2002) Model for intersegmental coordination of leech swimming: central and sensory mechanisms. J Neurophysiol 87:2760–2769.

Cruse H (1990) What mechanisms coordinate leg movement in walking arthropods? Trends Neurosci 13:15–21.

Daun S, Mantziaris C, Tóth T, Büschges A, Rosjat N (2019) Unravelling intra- and intersegmental neuronal connectivity between central pattern

generating networks in a multi-legged locomotor system. PLoS One 14: e0220767.
Daun-Gruhn S, Tóth TI (2011) An inter-segmental network model and its use in elucidating gait-switches in the stick insect. J Comput Neurosci 31:43–60.
David I, Holmes P, Ayali A (2016) Endogenous rhythm and pattern-generating circuit interactions in cockroach motor centres. Biol Open 5:1229–1240.
Delcomyn F (1991) Perturbation of the motor system in freely walking cockroaches. I. Rear leg amputation and the timing of motor activity in leg muscles. J Exp Biol 156:483–502.
Fuchs E, Holmes P, Kiemel T, Ayali A (2011) Intersegmental coordination of cockroach locomotion: adaptive control of centrally coupled pattern generator circuits. Front Neural Circuits 4:125.
Gabriel JP, Scharstein H, Schmidt J, Büschges A (2003) Control of flexor motoneuron activity during single leg walking of the stick insect on an electronically controlled treadwheel. J Neurobiol 56:237–251.
Grabowska M, Godlewska E, Schmidt J, Daun-Gruhn S (2012) Quadrupedal gaits in hexapod animals – inter-leg coordination in free-walking adult stick insects. J Exp Biol 215:4255–4266.
Graham D (1981) Walking kinetics of the stick insect using a low-inertia counter-balanced, pair of independent treadwheels. Biol Cybern 40:49–57.
Grillner S (2006) Biological pattern generation: the cellular and computational logic of networks in motion. Neuron 52:751–766.
Grillner S, El Manira A (2020) Current principles of motor control, with special reference to vertebrate locomotion. Physiol Rev 100:271–320.
Grillner S, Wallén P (1985) Central pattern generators for locomotion, with special reference to vertebrates. Annu Rev Neurosci 8:233–261.
Gruhn M, Rosenbaum P, Bockemühl T, Büschges A (2016) Body side-specific control of motor activity during turning in a walking animal. Elife 5: e13799.
Katz PS (2016) Evolution of central pattern generators and rhythmic behaviours. Philos Trans R Soc Lond B Biol Sci 371:20150057.
Knebel D, Ayali A, Pflüger H-J, Rillich J (2017) Rigidity and flexibility: the central basis of inter-leg coordination in the locust. Front Neural Circuits 10:112.
Laurent G, Burrows M (1988) A population of ascending intersegmental interneurones in the locust with mechanosensory inputs from a hind leg. J Comp Neurol 275:1–12.
Ludwar BC, Göritz ML, Schmidt J (2005) Intersegmental coordination of walking movements in stick insects. J Neurophysiol 93:1255–1265.
Mantziaris C, Bockemühl T, Büschges A (2020) Central pattern generating networks in insect locomotion. Dev Neurobiol 80:16–30.
Mantziaris C, Bockemühl T, Holmes P, Borgmann A, Daun S, Büschges A (2017) Intra- and intersegmental influences among central pattern generating networks in the walking system of the stick insect. J Neurophysiol 118:2296–2310.
Puhl JG, Mesce KA (2008) Dopamine activates the motor pattern for crawling in the medicinal leech. J Neurosci 28:4192–4200.
Ritzmann R, Zill SN (2013) Neuroethology of insect walking. Scholarpedia 8:30879.
Ronacher B, Wolf H, Reichert H (1988) Locust flight behavior after hemisection of individual thoracic ganglia: evidence for hemiganglionic premotor centers. J Comp Physiol 163:749–759.
Rosenbaum P, Wosnitza A, Büschges A, Gruhn M (2010) Activity patterns and timing of muscle activity in the forward walking and backward walking stick insect *Carausius mororsus*. J Neurophysiol 104:1681–1695.
Rosenbaum P, Schmitz J, Schmidt J, Büschges A (2015) Task-dependent modification of leg motor neuron synaptic input underlying changes in walking direction and walking speed. J Neurophysiol 114:1090–1101.
Schilling M, Cruse H (2020) Decentralized control of insect walking: a simple neural network explains a wide range of behavioral and neurophysiological results. PLoS Comput Biol 16:e1007804.
Schilling M, Hoinville T, Schmitz J, Cruse H (2013) Walknet, a bio-inspired controller for hexapod walking. Biol Cybern 107:397–419.
Schmidt J, Fischer H, Büschges A (2001) Pattern generation for walking and searching movements of a stick insect leg. II. Control of motoneuronal activity. J Neurophysiol 85:354–361.
Schmitz J (1993) Load-compensating reactions in the proximal leg joints of stick insects during standing and walking. J Exp Biol 183:15–33.
Schmitz J, Delcomyn F, Büschges A (1991) Oil and hook electrodes for en passant recordings from small nerves. Methods Neurosci 4:266–278.
Smarandache-Wellmann C, Grätsch S (2014) Mechanisms of coordination in distributed neural circuits: encoding coordinating information. J Neurosci 34:5627–5639.
Sponberg S, Full RJ (2008) Neuromechanical response of musculo-skeletal structures in cockroaches during rapid running on rough terrain. J Exp Biol 211:433–446.
Tóth TI, Daun S (2019) A kinematic model of stick-insect walking. Physiol Rep 7:e14080.
Toth TI, Grabowska M, Rosjat N, Hellekes K, Borgmann A, Daun-Gruhn S (2015) Investigating inter-segmental connections between thoracic ganglia in the stick insect by means of experimental and simulated phase response curves. Biol Cybern 109:349–362.
Weidler DJ, Diecke FPJ (1969) The role of cations in conduction in the central nervous system of the herbivorous insect *Carausius morosus*. Z Vergl Physiol 64:372–399.
Wosnitza A, Engelen J, Gruhn M (2013) Segment-specific and state-dependent targeting accuracy of the stick insect. J Exp Biol 216:4172–4183.
Zill SN, Keller BR, Chaudhry S, Duke ER, Neff D, Quinn R, Flannigan C (2010) Detecting substrate engagement: responses of tarsal campaniform sensilla in cockroaches. J Comp Physiol A Neuroethol Sens Neural Behav Physiol 196:407–420.
Zill SN, Dallmann CJ, Büschges A, Chaudhry S, Schmitz J (2018) Force dynamics and synergist muscle activation in stick insects: the effects of using joint torques as mechanical stimuli. J Neurophysiol 120:1807–1823.